Covalent polymer functionalization of graphene nanosheets and mechanical properties of composites

Ming Fang [a], Kaigang Wang [a], Hongbin Lu *[a], Yuliang Yang [a] and Steven Nutt [b]

[a]*The Key Laboratory of Molecular Engineering of Polymers of Ministry of Education, Department of Macromolecular Science, Fudan University, Shanghai, 200433, China.;* [b]*Department of Chemical Engineering and Materials Science, University of Southern California, Los Angeles, CA 90089-0241, USA*

*E-mail: hongbinl@fudan.edu.cn. Fax: +86-21-55664589; Tel: +86-21-55664589

Abstract: For developing high performance graphene-based nanocomposites, dispersal of graphene nanosheets in polymer hosts and precise interface control are challenging due to their strong interlayer cohesive energy and surface inertia. Here we report an efficient method to functionalize graphene nanosheets. The initiator molecules were covalently bonded to the graphene surface *via* a diazonium addition and the succeeding atom transfer radical polymerization linked polystyrene chains (82 wt% grafting efficiency) to the graphene nanosheets. The prominent confinement effect arising from nanosheets resulted in a 15 °C increase in the glass transition temperature of polystyrene compared to the pure polymer. The resulting polystyrene nanocomposites with 0.9 wt% graphene nanosheets revealed around 70% and 57% increases in tensile strength and Young's modulus. The protocol is believed to offer possibilities for optimizing the processing properties and interface structure of graphene-polymer nanocomposites.

1. Introduction

Graphene has opened new pathways for developing a wide range of novel functional materials.[1] Excellent properties and inexpensive sources (graphite) have spurred intensive interest

Please cite this article as: M. Fang, K. Wang, H. Lu, Y. Yang, and S. R. Nutt, **"Covalent Polymer Functionalization of Graphene Nanosheets and Mechanical Properties of Composites"**, J. Mater. Chem. 19 (2009) 7098-7105. DOI:**http://dx.doi.org/10.1039/b908220d**

in developing cost-effective, high-performance polymernanocomposites.[2] Recent studies have demonstrated intriguing attributes of graphene, including high thermal conductivity,[3] mechanical strength comparable to carbon nanotubes,[1e] superior transport properties[4] and giant thermoelectric effect.[5] To fully exploit these properties, graphene can be incorporated into polymer matrices. However, this must be done judiciously, as delicate morphological organization, fine interface control, uniform dispersion, and ease of processing are essential to the performance of the resulting composites.[6] These requisites stem largely from the surface properties of graphene, which can be chemically modified for specific purposes. For example, surfactants[7] and polyelectrolytes[8] have been used to enhance exfoliation and dispersion of graphene in various media through physical or electrostatic interactions. Using a different approach, organic molecules, *e.g.*, phenyl isocyanate[2a,9] and porphyrin[10] *etc*., have also been attached to graphene surfaces to improve dispersion in non-polar polymers such as polystyrene. However, to achieve stable dispersions of graphene and optimize the microstructure of nanocomposites, polymer functionalization of the graphene surface is often necessary.[6] Here we report a covalently-bonded, polymer-functionalized graphene hybrid material, achieved by combining a diazonium addition reaction with atom transfer radical polymerization (ATRP). Functionalization resulted in 82 wt% polymer grafting efficiency and a 15 °C increase in the glass transition temperature (T_g) compared to the pure polymer. By dispersing such functionalized graphene nanosheets in polystyrene films we demonstrate mechanical improvements as high as ~70% and ~57% increases in tensile strength and Young's modulus. This is almost comparable to the reinforcement effect of carbon nanotubes.[11]

Functionalization of graphene nanosheets affects the total free energy of mixture systems, which consists of enthalpic and entropic contributions.[12]Graphene oxide, often used as a starting material

Please cite this article as: M. Fang, K. Wang, H. Lu, Y. Yang, and S. R. Nutt, **"Covalent Polymer Functionalization of Graphene Nanosheets and Mechanical Properties of Composites"**, J. Mater. Chem. 19 (2009) 7098-7105. DOI:**http://dx.doi.org/10.1039/b908220d**

in the production of reduced graphene nanosheets, possesses hydroxyl and epoxide groups attached on the basal plane, and carboxyl groups at the edge.[1] The presence of polar groups facilitates the dissolution of graphene oxide nanosheets in water and polar solvents such as DMF.[13] In such cases, the dispersion stability of graphene oxide is dictated primarily by enthalpic interaction between graphene oxide and solvents. In contrast, (reduced) graphene nanosheets are highly hydrophobic, and the interlayer cohesive energy (van der Waals interaction) increases sharply with increasing sheet size. This increase usually results in irreversible aggregation without electrostatic or steric protection.[14] Grafting polymers can prevent aggregation of graphene sheets by significantly reducing the enthalpic interaction so that the dispersion in polymers is primarily driven by the system entropy. During mixing, the graphene-polymer size ratio and the molecular weight of grafting polymers play key roles in the dispersion ofgraphene.[15] In the present work, we functionalize individual and multi-layer graphene sheets (size range: 20–40 nm) with linear polystyrene (PS, number average molecular weight: ~60000, average square radius of gyration R_g ($0.028 \times \sqrt{M} \approx 7$ nm). Reducing the nanosheet size decreases the interlayer cohesive energy, reduces the viscosity of solution or melt mixtures, and limits the introduction of excess free volume in the system.[15–17] In addition, the ATRP protocol used affords convenient control of the thickness and molecular structure of the graphene-host interface,[18] which creates a fundamental route for further understanding of the reinforcement mechanism of graphene nanocomposites.

2. Experimental

2.1. Materials

Graphite powder (120 μm) was purchased from Qingdao BCSM CO. LTD. Dimethylformamide (DMF), 98% H_2SO_4, 30% H_2O_2, 50% hydrazine hydrate, CuBr and $KMnO_4$ were purchased from

Please cite this article as: M. Fang, K. Wang, H. Lu, Y. Yang, and S. R. Nutt, **"Covalent Polymer Functionalization of Graphene Nanosheets and Mechanical Properties of Composites"**, J. Mater. Chem. 19 (2009) 7098-7105. DOI:**http://dx.doi.org/10.1039/b908220d**

Shanghai Zhenxin Chemical Company. Styrene (St), N,N,N′,N′,N″-pentamethyl-diethylenetriamine (PMDETA), 2-(4-aminophenyl)ethanol, isoamyl nitrite, triethanolamine, 2-bromopropionyl bromide, 1,2-dichloro-benzene (DCB), tetrahydrofuran (THF) and 2-bromo-propionate (MBP) were purchased from Alfa Aesar. CuBr (95%) was stirred overnight in acetic acid, filtered, washed with ethanol and diethyl ether successively, and dried under vacuum. St was dried using $CaCl_2$ for 48 h and distilled before use. Polystyrene (Sigma-Aldrich) used to prepare nanocomposite films has a number average molecular weight of 139000 and a polydispersity of 2.5. Other materials were used as received.

2.2. Synthesis and purification of graphite oxide (GO)

GO was prepared using a modification of Hummers and Offeman's method.8,19 In a typical reaction, 5 g graphite, 5 g $NaNO_3$, and 230 mL H_2SO_4 were stirred together in an ice bath. $KMnO_4$ (15 g) was slowly added while stirring, and the rate of addition was controlled to prevent the mixture temperature from exceeding 20 °C. The mixture was then transferred to a 35 °C water bath and stirred for about 0.5 h, forming a thick paste. Subsequently, 230 mL de-ionized water was added gradually, causing an increase in temperature to 98 °C. After 15 min, the mixture was further treated with 700 mL de-ionized water and 50 mL 30% H_2O_2 solution. The warm solution was then filtered and washed with de-ionized water until the pH was 7 and dried at 65 °C under vacuum.

2.3. Synthesis of graphene-OH

Diazonium addition: in a typical experiment,[18] 1 g GO was loaded in a 500 mL round-bottom flask and 250 mL de-ionized water was then added. After stirring and ultrasonication for 30 min, 5 mL 50% hydrazine hydrate was gradually added to the solution. Subsequently, the mixture was transferred to a 100 °C oil bath and stirred for 4 h. 4 g 2-(4-aminophenyl)ethanol and 3 mL isoamyl

Please cite this article as: M. Fang, K. Wang, H. Lu, Y. Yang, and S. R. Nutt, **"Covalent Polymer Functionalization of Graphene Nanosheets and Mechanical Properties of Composites"**, J. Mater. Chem. 19 (2009) 7098-7105. DOI:**http://dx.doi.org/10.1039/b908220d**

nitrite were then added. The mixture was stirred vigorously at 80 °C overnight and then cooled to room temperature and filtered using a Teflon filter (0.2 μm). The filter cake was washed with de-ionized water and DMF until the filtrate was clear. The remaining black solid was dried under vacuum.

2.4. Synthesis of graphene initiator

All operations were carried out under nitrogen atmosphere. 0.5 g graphene-OH was added to 10 mL THF, to which 0.9 mL triethanolamine was then added. After the solution was cooled to 0 °C, 0.43 g (2 mmol) 2-bromopropionyl bromide was added dropwise. The mixture was stirred for 2 h at 0 °C followed by stirring at room temperature for 24 h. The solid was then separated from the mixture by filtration and washed with water 5 times. The raw product was re-dispersed in 20 mL THF and the same dispersing, filtering and washing steps were repeated three times to remove the adsorbed, unreacted organic molecules. The black filtered solid was collected and dried overnight under vacuum at 40 °C.

2.5. Synthesis of graphene-PS

Typically, 0.5 g graphene-initiator, 83.5 mg methyl-2-bromopropionate (MBP), 10.4 g St and 30 mg CuBr (0.2 mmol) were dissolved in 8 mL 1,2-dichlorobenzene (DCB). The mixture was degassed by three freeze-pump-thaw cycles, after which 0.0417 mL PMEDTA (0.2 mmol) was added using a syringe. The flask was immersed immediately in an oil bath at 110 °C and stirred for 10 h. At the end of the reaction, the viscosity had increased dramatically. The mixture was diluted with THF and filtered with a Teflon filter (0.2 μm). The filtrate was passed through a column chromatograph filled with neutral alumina to remove the copper complex, and precipitated in 200 mL methanol. Subsequently, the product was purified by dissolution/precipitation twice with methanol, and dried

Please cite this article as: M. Fang, K. Wang, H. Lu, Y. Yang, and S. R. Nutt, **"Covalent Polymer Functionalization of Graphene Nanosheets and Mechanical Properties of Composites"**, J. Mater. Chem. 19 (2009) 7098-7105. DOI:**http://dx.doi.org/10.1039/b908220d**

at 40 °C in vacuum for 17 h. After washing the gray solid with 100 mL DMF three times, the resulting black solid was dried under vacuum at 40 °C.

2.6. Preparation of PS and graphene-PS films

All film samples were prepared by a solution drop-casting method. Different mass fractions of graphene-PS particles were dispersed in toluene with the assistance of sonication at room temperature. These solutions were mixed with toluene solutions containing 15 wt% PS and sonicated for an additional 30 min at room temperature to remove air bubbles trapped in solution. The obtained homogeneous solutions were slowly dropped onto cleaned glass dishes and dried in vacuum for 72 h at 50 °C and overnight at 100 °C. The resulting films were peeled off the substrate for mechanical testing.

2.7. Characterization

Atomic force micrographs (AFM) were acquired using a Multimode Nano 4 in the tapping mode. The set-point amplitude ratio was maintained at 0.9 to minimize the deformation caused by the tip. For AFM observations, the graphene dispersions (0.1 mg/ml in DMF) were treated with ultrasonication and then spin-coated onto a freshly cleaved mica surface. The interlayer spacings of graphite and graphene samples were measured using a Rigaku D/max-γB X-ray diffractometer with Cu Kα radiation (λ = 1.54 Å); the X-ray scanning rate was 0.02 degrees per second ranging from 5 to 60°. The average molecular weight of PS was determined by gel permeation chromatography (GPC, Waters Breeze, USA); THF was used as an eluent and narrow PS standard for calibration. Fourier transform (FTIR) spectra were recorded on a NEXUS 670 spectrometer. Raman spectra were measured on a Dilor LABRAM-1B multi-channel confocal microspectrometer with 631 nm laser excitation. Thermogravimetric analysis (TGA, Netzsch TG 209) was conducted in a nitrogen

Please cite this article as: M. Fang, K. Wang, H. Lu, Y. Yang, and S. R. Nutt, **"Covalent Polymer Functionalization of Graphene Nanosheets and Mechanical Properties of Composites"**, J. Mater. Chem. 19 (2009) 7098-7105. DOI:**http://dx.doi.org/10.1039/b908220d**

atmosphere from ambient temperature to 700 °C with a heating rate of 20 °C/min. Before all tests, samples were ground to ensure uniform heat diffusion and 6–10 mg samples were used for each test. Differential scanning calorimetry (DSC, TA Q100) was performed in a nitrogen atmosphere from room temperature to 160 °C at 10 °C/min. The data were recorded after erasing the previous thermal history and the glass transition temperature (T_g) was determined from the midpoint of the transition steps. The mechanical properties of graphene-PS nanocomposites were measured using a universal testing machine (CMT-4102, SANS Group, China) at room temperature. A load cell of 500 N was employed and the tensile rate imposed was 1 mm/min. All samples were cut into the dumbbell shape with a razor blade. More than five tests were conducted for each sample, from which the mean values and standard deviations were derived.

3. Results and discussion

A typical procedure for preparing polystyrene-functionalized graphene nanosheets is presented in Scheme 1. The three-step process includes (1) graphene oxide preparation by means of the modified Hummers and Offeman method,[8,19] (2) grafting of the ATRP initiator to the reduced graphene surface, and (3) in-situ polymerization of styrene in the presence of graphene sheets. Note that for successful polymer functionalization, the interlayer cohesive energy of exfoliated graphene (oxide) nanosheets must be carefully controlled during processing. The oxygen functionalities of hydroxyl and epoxide groups on the basal planes of graphene oxide sheets can be compromised during reduction, depending on the extent of reduction (hydrazine hydrate is used in the present work). This foments a strong tendency for aggregation. The aggregation tendency can be reduced by decreasing the size of graphene nanosheets (since the van de Waals interparticle adhesion energy decreases with R, the particle radius14) or by employing surfactants such as sodium dodecylbenzene sulfonate

Please cite this article as: M. Fang, K. Wang, H. Lu, Y. Yang, and S. R. Nutt, **"Covalent Polymer Functionalization of Graphene Nanosheets and Mechanical Properties of Composites"**, J. Mater. Chem. 19 (2009) 7098-7105. DOI:**http://dx.doi.org/10.1039/b908220d**

(SDBS). The use of surfactants requires additional removal steps to optimize the interface structure. In our experiments, we found that relatively small, hydrazine-reduced graphene nanosheets (20–40 nm in diameter) were readily dispersed in water without surfactants. Dispersal was assisted by the electrostatic repulsive force arising from residual carboxyl groups at graphene sheet edges, and by the weakened interparticle interaction. Such surfactant-free, reduced graphene dispersion in water or organic solvents is desirable for subsequent diazonium addition and styrene polymerization at the basal plane.

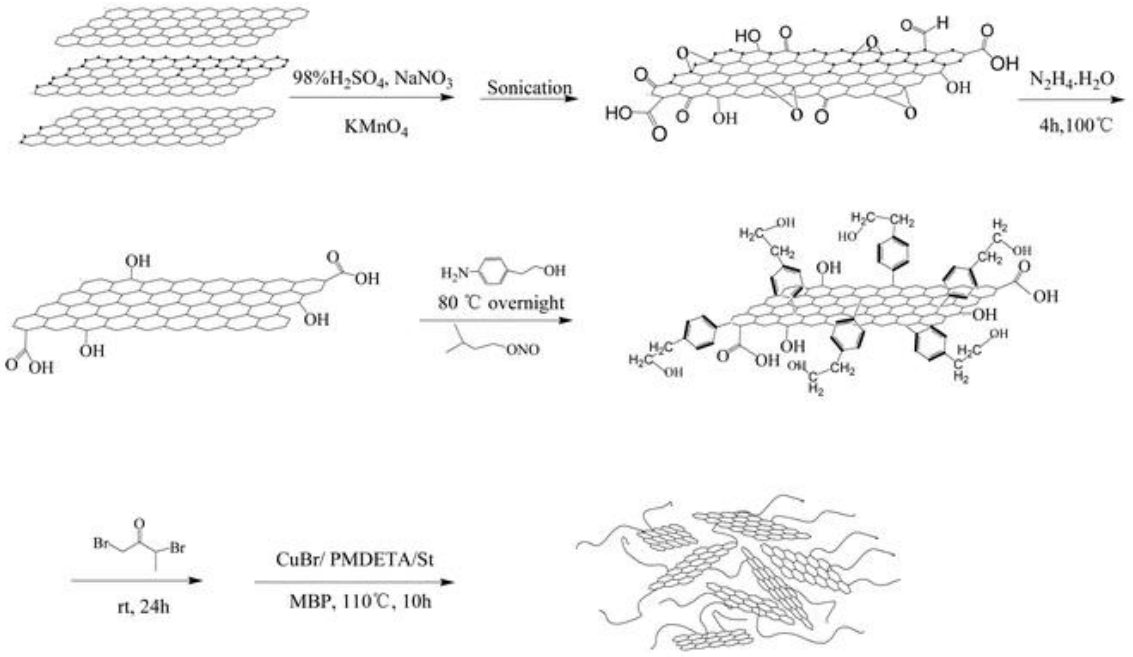

Scheme 1 Synthesis route of polystyrene-functionalized graphene nanosheets.

Diazonium addition reaction has been employed to functionalize single-walled carbon nanotubes and to enhance the dispersion of graphene in organic solvents such as DMF.[18] Here we exploit the same approach to link the radical initiator to the graphene surface. Subsequent in-situ polymerization allows polystyrene chains to be grafted to the nanosheet surface. The covalent link between graphene sheets and PS chains was confirmed by optical spectroscopy. Fig. 1 shows Raman spectra of the

Please cite this article as: M. Fang, K. Wang, H. Lu, Y. Yang, and S. R. Nutt, **"Covalent Polymer Functionalization of Graphene Nanosheets and Mechanical Properties of Composites"**, J. Mater. Chem. 19 (2009) 7098-7105. DOI:**http://dx.doi.org/10.1039/b908220d**

graphite and graphene sheets. A laser excitation of 631 nm was used, and all powder samples were directly deposited on the wafer in the absence of solvents. In all samples, two prominent peaks are clearly visible, corresponding to the so-called D and G bands at 1333 and 1582 cm^{-1}, respectively.[20] The D band arises from the activation in the first order scattering process of sp^3 carbons in graphene sheets, and the intensity ratio of D and G bands expresses the sp^2/sp^3carbon ratio, a measure of the extent of disorder.[20a] For our samples, the D/G ratios of the graphite oxide, initiator-grafted, and PS-grafted graphene sheets are respectively 1.73, 1.71 and 1.02, reflecting the increase in disorder after diazonium addition. Generally, the D band is relatively weak or nearly invisible for perfect graphene lattices, which arises primarily from symmetry breaking at the edge.[21] The D band adsorption observed for the pristine graphite used in our experiments thus indicates the presence of defects. Such disorder is also reflected in the broadened and blue-shifted (higher frequency) G bands for the graphite oxide and the two graphene samples.[20] As shown in Fig. 1, the G band of the graphite oxide appears at 1595 cm^{-1}, which is 15 cm^{-1} higher than that of pristine graphite (1580 cm^{-1}). After reduction of graphite oxide with hydrazine, the vibration frequency of the G band decreases to 1585 cm^{-1}, slightly higher than that of graphite oxide. A similar phenomenon was reported by Kudin et al., who attributed this to the influence of defects and isolated double bonds.[20a] Although reduced graphite oxide reportedly indicates an increased D/G ratio (relative to graphite oxide),[22] the change in the D/G ratio can be at least partly attributed to the formation of covalent bonds between graphene and initiator and/or PS chains.

Please cite this article as: M. Fang, K. Wang, H. Lu, Y. Yang, and S. R. Nutt, **"Covalent Polymer Functionalization of Graphene Nanosheets and Mechanical Properties of Composites"**, J. Mater. Chem. 19 (2009) 7098-7105. DOI:**http://dx.doi.org/10.1039/b908220d**

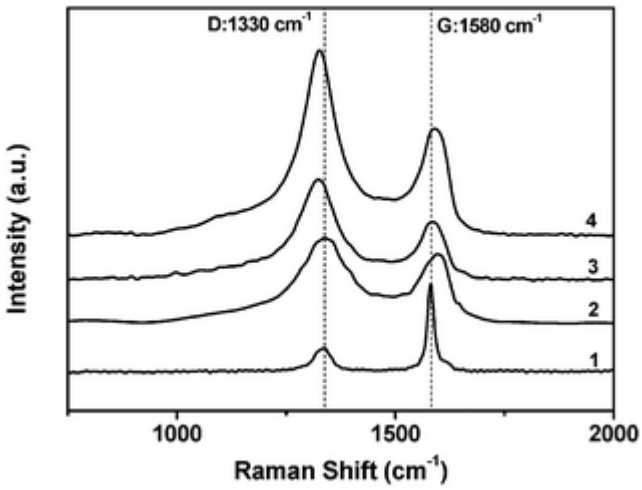

Fig. 1 Raman spectra of the pristine graphite (1), graphite oxide (2), graphene-initiator (3) and graphene-PS (4), with a laser excitation wavelength of 631 nm.

Further evidence of covalent bonding between graphene and PS chains is provided by the Fourier transform infrared (FTIR) spectra shown in Fig. 2. The FTIR spectrum from the initiator-grafted graphene sheets exhibits two characteristic peaks at 1740 and 1160 cm^{-1}, indicating the presence of the ester bond formed by reaction between graphene-OH and 2-bromopropionyl bromide.[23] However, these two peaks are much weaker in the spectrum of graphene-PS due to the shielding effect of PS chains grafted to the graphene. Multiple characteristic adsorption peaks are evident in the spectrum from the graphene-PS sample (note that this sample was exhaustively washed to remove the free PS chains adsorbed on the graphene prior to the FTIR tests). Four strong peaks at 700, 754, 1480 and 1490 cm^{-1} correspond to absorptions of the benzene ring of PS segments, while the peaks at 2920 and 3030 cm^{-1} arise from the attachment of additional methylene groups.[24] Because the PS chains grow only from the initiator grafted to the graphene surface (free PS chains in tested samples were removed by exhaustive washing), these FTIR results provide direct evidence for covalent bonding between graphene and PS chains. In addition, variation in the peak intensity around 3450 cm^{-1} reflects the effect of PS chains grafted on the graphene surface on the

Please cite this article as: M. Fang, K. Wang, H. Lu, Y. Yang, and S. R. Nutt, **"Covalent Polymer Functionalization of Graphene Nanosheets and Mechanical Properties of Composites"**, J. Mater. Chem. 19 (2009) 7098-7105. DOI:**http://dx.doi.org/10.1039/b908220d**

hydroxyl absorption. For convenience of comparison, the amount of C–Br bonds (538 cm^{-1}) on the graphene surface is assumed to be the same,[25] which allows us to normalize FTIR spectrum of the graphene-PS sample. Again, remarkably reduced hydroxyl absorption (3450 cm^{-1}) indicates a shielding effect of PS chains. In this regard, we need to note that the assumption of identical numbers of C–Br bonds in these two samples actually overestimates the FTIR contribution of C–Br bonds in the graphene-PS sample in view of the shielding effect of PS, likewise.[26] This implies that normalization treatment could amplify the absorption intensity of hydroxyl groups in the graphene-PS sample. Nevertheless, the hydroxyl absorption in graphene-PS is still weaker than that in graphene-initiator sample. This affords further support for covalent bonding at the interface. Next, we quantify the polystyrene grafted to the graphene sheets, and examine the segmental relaxation behavior.

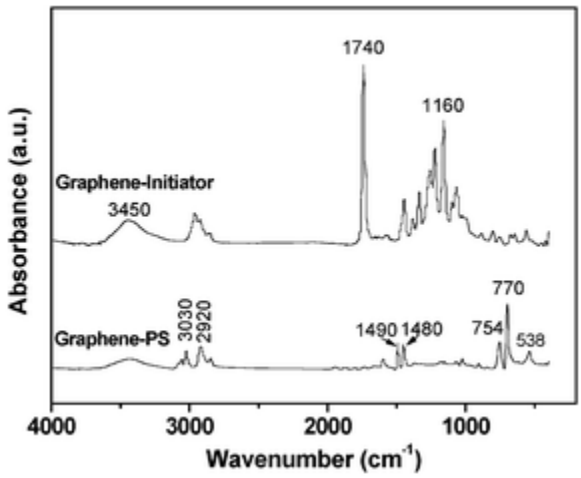

Fig. 2 *FTIR spectra of the graphene-initiator and PS-grafted graphene in which the spectrum of the graphene-PS sample was normalized using the intensity of the 538 cm^{-1} peak (C–Br stretching vibration, assuming an identical number of C–Br bonds in two samples) to eliminate the effect of the amount of samples employed in tests.*

Please cite this article as: M. Fang, K. Wang, H. Lu, Y. Yang, and S. R. Nutt, **"Covalent Polymer Functionalization of Graphene Nanosheets and Mechanical Properties of Composites"**, J. Mater. Chem. 19 (2009) 7098-7105. DOI:**http://dx.doi.org/10.1039/b908220d**


Fig. 3 shows thermogravimetric curves from the graphite oxide and the two graphene samples. Graphite oxide is not thermally stable, and mass loss started below 100 °C and was rapid at 150 °C. Similar results were reported by Stankovich et al.,[22] who attributed mass loss in the early stage (<100 °C) to the pyrolysis of labile oxygen-containing groups such as –OH, COOH etc. The lower starting temperature for rapid mass loss reported here (150 °C versus 200 °C) reflects the higher defect density present in our graphite oxide samples, although our heating rate is also considerably greater (20 versus 5 °C/min).[22] A decrease in defect density would improve the thermal stability of graphite and/or graphene sheets. This assertion is consistent with the thermal behavior of 2-(4-aminophenyl)ethanol-grafted graphene sheets (graphene-OH), which were subjected to hydrazine reduction for up to 4 hours in a 100 °C refluxed aqueous solution prior to the grafting. In contrast, polymer coatings appear to be more effective for enhancing thermal stability of graphene sheets. For example, the maximum mass loss temperature (~350 °C) of graphene-PS sheets was roughly 200 °C higher than that of graphite oxide. Assuming that the weight loss that occurred during thermal decomposition of the graphene-PS sample was due entirely to the removal of the grafted PS layer, the residual weight after the decomposition (18 wt%) implies a polymer graft content as high as 82 wt%. With GPC the molecular size of these graft PS chains was determined by measuring the free polymer simultaneously produced during grafting polymerization.[27] The results indicate that the number average molecular weight and polydispersity index of graft PS are 60000 and 1.6, respectively. Because of the presence of graphene sheets, these covalently grafted PS chains will show some confined dynamic behavior different from the pristine polymer, which is discussed below.

Please cite this article as: M. Fang, K. Wang, H. Lu, Y. Yang, and S. R. Nutt, **"Covalent Polymer Functionalization of Graphene Nanosheets and Mechanical Properties of Composites"**, J. Mater. Chem. 19 (2009) 7098-7105. DOI:**http://dx.doi.org/10.1039/b908220d**

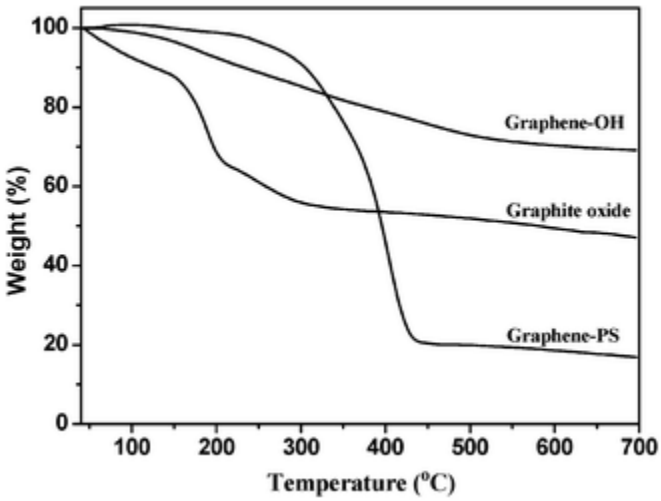

Fig. 3 TGA curves of the graphite oxide, 2-(4-aminophenyl)ethanol-grafted graphene (graphene-OH) and PS-graftedgraphene, with a heating rate of 20 °C/min in nitrogen.

The relaxation behavior of polymer chains grafted to the solid surface is distinct from that of free or entangled chains, and this difference can indirectly indicate the type of interaction between phases, such as covalent bonding.[6c,28] The segmental dynamics of polymers is essentially cooperative and is strongly influenced by embedded particles. The glass transition, T_g, is a macroscopic indication of the relaxation behavior of nanocomposite systems, and its magnitude depends on multiple structural parameters. For graphene-based composites, the T_g of polyacrylonitrile (PAN) was reportedly increased by 40 °C with the addition of only 1 wt% oxygenated graphene sheets, a phenomenon attributed to a strong particle-polymer interaction.[2b] A recent report claimed that the T_g of PS-based composites could be tailored by precisely controlling the size of the grafting polymer and particles, the grafting density, and the particle loading.[13a] Compared with polar polymers such as PAN, the influence of incorporated particles on the T_g of non-polar polymers like PS is generally weak. Therefore, a ~10 °C increase in T_g for the PS composite with 1.5 wt% PS-coated gold nanoparticles (diameter 5 nm) represents a substantial enhancement.[14a] Similarly, Fig. 4 reveals a 15 °C increase in T_g for the PS composite containing 12

Please cite this article as: M. Fang, K. Wang, H. Lu, Y. Yang, and S. R. Nutt, **"Covalent Polymer Functionalization of Graphene Nanosheets and Mechanical Properties of Composites"**, J. Mater. Chem. 19 (2009) 7098-7105. DOI:**http://dx.doi.org/10.1039/b908220d**

wt% graphene sheets. Note that all samples used for DSC measurements were produced by precipitation from the corresponding solutions, and thus the PS chains in these samples were not highly entangled. The increased T_g of the composite is thus attributed to the strong confinement effect of graphene sheets on the PS chains, and involves covalent bonding. In this regard, a quantitative equivalence between polymer composites and thin polymer films has been proposed to better understand the confinement effect.[29] Recent neutron scattering experiments have suggested a bulk behavior for a PS film thicker than 4Rg, which implies that PS chains in an interface layer thinner than $4R_g$ ($4 \times 0.028 \times \sqrt{M} \approx 28$ nm) would experience such a confinement effect from substrates or particles.[30]

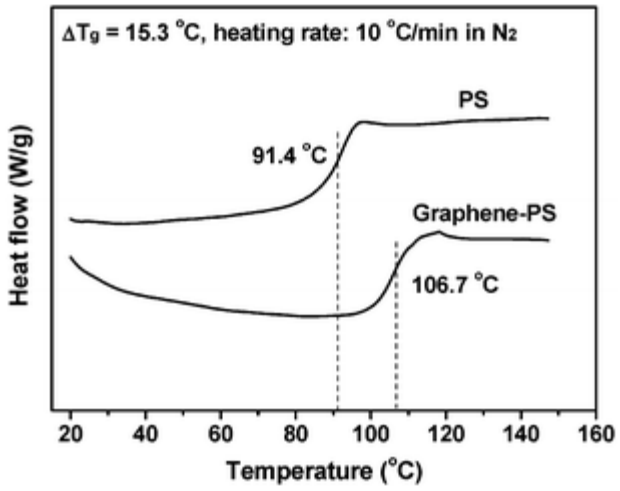

Fig. 4 DSC curves of the neat PS and PS-grafted graphene; the measurements were conducted after removing thermal history (second scans).

Atomic force microscopy (AFM) provides a measure of the thickness of the interface layer grafted on the graphene surface. Fig. 5(left) shows AFM images of the initiator-grafted graphene sheets, revealing uniformly distributed nanosheets 20–40 nm in diameter. When the size of the small initiator molecules is neglected, the observed morphology reflects the approximate dimensions of

Please cite this article as: M. Fang, K. Wang, H. Lu, Y. Yang, and S. R. Nutt, **"Covalent Polymer Functionalization of Graphene Nanosheets and Mechanical Properties of Composites"**, J. Mater. Chem. 19 (2009) 7098-7105. DOI:**http://dx.doi.org/10.1039/b908220d**

the graphene sheets. A thickness of ~0.73 nm is consistent with the reported value,[2] indicating that these nanosheets are well-exfoliated graphene. In contrast, Fig. 5(right) shows the morphology of the PS-grafted graphene sheets. The size and shape of the PS-graphene differed from the initiator-graphene (Fig. 5(left)), spanning a larger size range (30–150 nm) and exhibiting more elliptical sheets. The average thickness is ~3 nm, with the exception of occasional larger sheets that were 250 × 150 × 7 nm. If we assume that the 3 nm nanosheets consist of an individual graphene sheets 0.73 nm thick, then we can deduce that the PS interface layers on the surfaces of the graphene sheets are ~1 nm. Apparently, this thin grafting layer experiences a strong relaxation confinement, in light of the $4R_g$ size concept described above. Carefully observing the PS-grafted graphene (Fig. 6), a mound-type distribution of PS chains on the graphene surface can be seen (note its width-height ratio is 133:3.6), that is, the thickness at the central area is higher than that at the peripheral area. This implies that the central PS chains adopted a more stretched conformation than those chains located at the periphery. In view of its lateral size larger than that of graphene-initiator sheets, those PS chains at the edge were supposed to roll out on the mica surface while those chains close to the center along the radial direction partially stack above the outmost chains. This will cause a density distribution of PS chains along the radial direction. Fig. 7 shows such a density difference between the central and peripheral areas of PS-grafted graphene sheets. Some sporadic black points on the periphery of PS-graphene sheets (as denoted by arrows) should not be considered because they are supposed to be fragments of filter paper. The average lateral size of PS-graphene sheets shown in the TEM image is around 100 nm and the color difference between the central and peripheral areas for each sheet reflects the different stacking densities of PS chains. This is consistent with the result of AFM observation.

Please cite this article as: M. Fang, K. Wang, H. Lu, Y. Yang, and S. R. Nutt, **"Covalent Polymer Functionalization of Graphene Nanosheets and Mechanical Properties of Composites"**, J. Mater. Chem. 19 (2009) 7098-7105. DOI:**http://dx.doi.org/10.1039/b908220d**

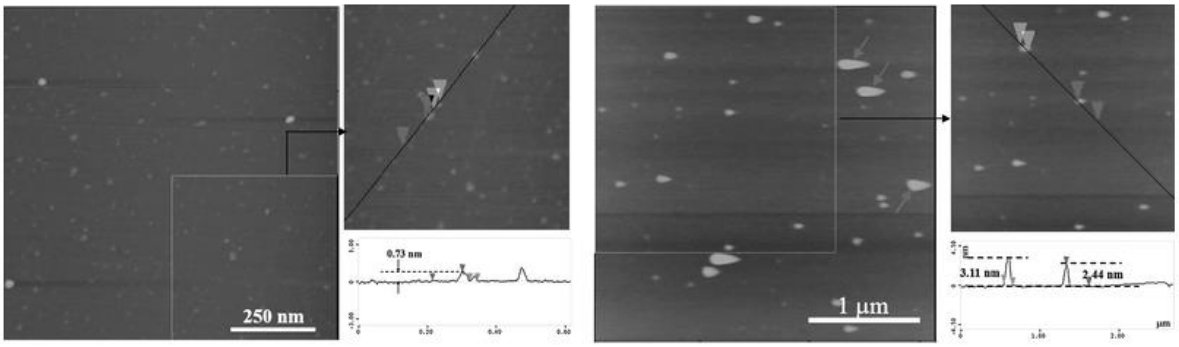

Fig. 5 Tapping mode AFM images of the initiator- (left) and PS-grafted (right) graphene.

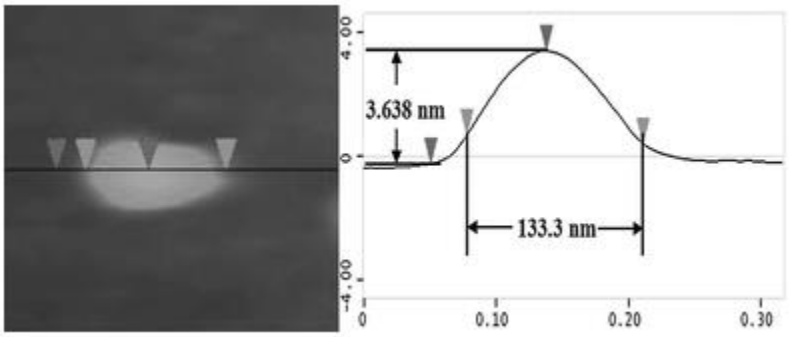

Fig. 6 Amplified AFM image of a PS-grafted graphene sheet (left); the lateral and thick sizes (right) corresponding to the PS-grafted graphene sheet shown on the left.

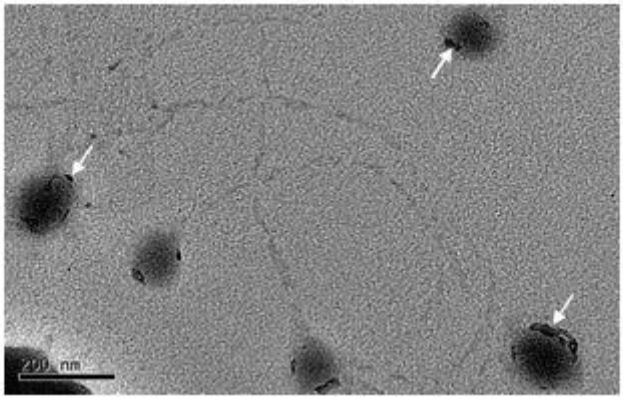

***Fig. 7** TEM image of PS-grafted graphene sheets.*

Apart from the PS-graphene sheets with the diameter of ~100 nm, some larger PS-graphene sheets can be seen in Fig. 5(right). The height measurement gives their thickness as around 7 nm. This implies that slight aggregation of graphene sheets could take place during the polymerization.

Please cite this article as: M. Fang, K. Wang, H. Lu, Y. Yang, and S. R. Nutt, **"Covalent Polymer Functionalization of Graphene Nanosheets and Mechanical Properties of Composites"**, J. Mater. Chem. 19 (2009) 7098-7105. DOI:**http://dx.doi.org/10.1039/b908220d**

Fig. 8 provides X-ray diffraction patterns from graphene and pristine graphite powder samples. The strong peak at 26.52° in the pristine graphite pattern was not present in the graphite oxide pattern, which showed a strong peak at 8.03° and a weak, broad peak at 16.88°. The latter two peaks indicate the presence of functional groups containing oxygen, which formed during oxidation. The groups cause the graphite oxide sheets to stack more loosely, and the interlayer spacing increases from 0.34 nm (26.52°) to 1.08 nm (8.03°). The covalent grafted initiator and PS chains facilitate the exfoliation of reduced graphene sheets (the strong peaks at 26.52 and 8.03° disappeared). However, several broad peaks at 21.53, 19.6 and 10.73° appeared in the graphene-initiator and graphene-PS sheets, indicating that aggregation persisted to some extent in these samples. Such aggregation is supposed to arise from the strong van der Waals interaction between the reduced graphene sheets. Although the interaction can be markedly decreased by tailoring the size of graphene sheets, contact between neighboring graphene sheets is unavoidable in the presence of shear forces that arise from stirring during the grafting reaction. In the absence of external disturbances (e.g., from sonication) and sufficient electrostatic repulsion, graphene aggregation may be retained during polymerization, yielding single- and multi-layer graphene sheets in the final PS-grafted product.

Please cite this article as: M. Fang, K. Wang, H. Lu, Y. Yang, and S. R. Nutt, **"Covalent Polymer Functionalization of Graphene Nanosheets and Mechanical Properties of Composites"**, J. Mater. Chem. 19 (2009) 7098-7105. DOI:**http://dx.doi.org/10.1039/b908220d**

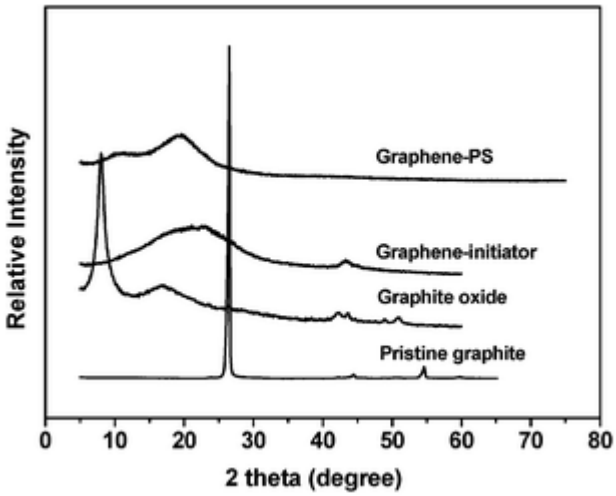

Fig. 8 XRD curves of the pristine graphite, graphite oxide, initiator- and PS-grafted graphene.

Given the excellent elastic modulus (~1100 GPa) and intrinsic strength (125 GPa) of graphene sheets,[1] we examine the effect of functionalized graphene sheets on the mechanical properties of PS films. These films were prepared by a typical drop-casting procedure, see the experimental section. The matrix used was PS (Sigma-Aldrich) with number average molecular weight of 139000 and polydispersity of 2.5. The samples used for measurement are shown in Fig. 9. At the low graphene content of 0.1 wt%, the composite film is light gray but the color of the samples (0.5 and 0.9 wt%) becomes black rapidly as the content of graphene sheets reached 0.5 wt% or more. Note that the amount of grafted PS was not included in the weight fraction of graphene sheets, that is, 82 wt% of PS in PS-grafted graphene sheets has been deducted for the denoted graphene contents of PS nanocomposites. Fig. 10(A) presents the representative stress-strain curves of the pristine PS and nanocomposite films. The pristine PS revealed a typical yield behavior with increasing stress during tension and the corresponding Young's modulus (EY) and fracture strength (σs) are 1.45 GPa and 24.44 MPa, respectively, see Fig. 10(B). The addition of graphene sheets remarkably changed the tensile behavior of PS films: yielding became hardly discernable especially at high graphene

Please cite this article as: M. Fang, K. Wang, H. Lu, Y. Yang, and S. R. Nutt, **"Covalent Polymer Functionalization of Graphene Nanosheets and Mechanical Properties of Composites"**, J. Mater. Chem. 19 (2009) 7098-7105. DOI:**http://dx.doi.org/10.1039/b908220d**

contents and the elongation at break decreased gradually. However, the EY and σs of nanocomposite films exhibited a remarkable increasing tendency. For the nanocomposite film with 0.9 wt% of graphene sheets, the EY and σs increased by 2.28 GPa and 41.42 MPa, corresponding to increases of 57.2 and 69.5%, respectively (relative to the pristine PS film).

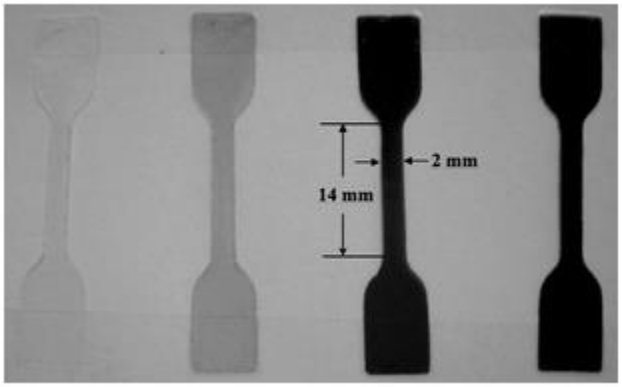

Fig. 9 *Appearance of dumbbell-type samples of the pristine PS and nanocomposite films. The data marked denote the dimensional size used for tensile tests: 14 × 2 × 0.07(±0.01) mm^3.*

Please cite this article as: M. Fang, K. Wang, H. Lu, Y. Yang, and S. R. Nutt, **"Covalent Polymer Functionalization of Graphene Nanosheets and Mechanical Properties of Composites"**, J. Mater. Chem. 19 (2009) 7098-7105. DOI:**http://dx.doi.org/10.1039/b908220d**

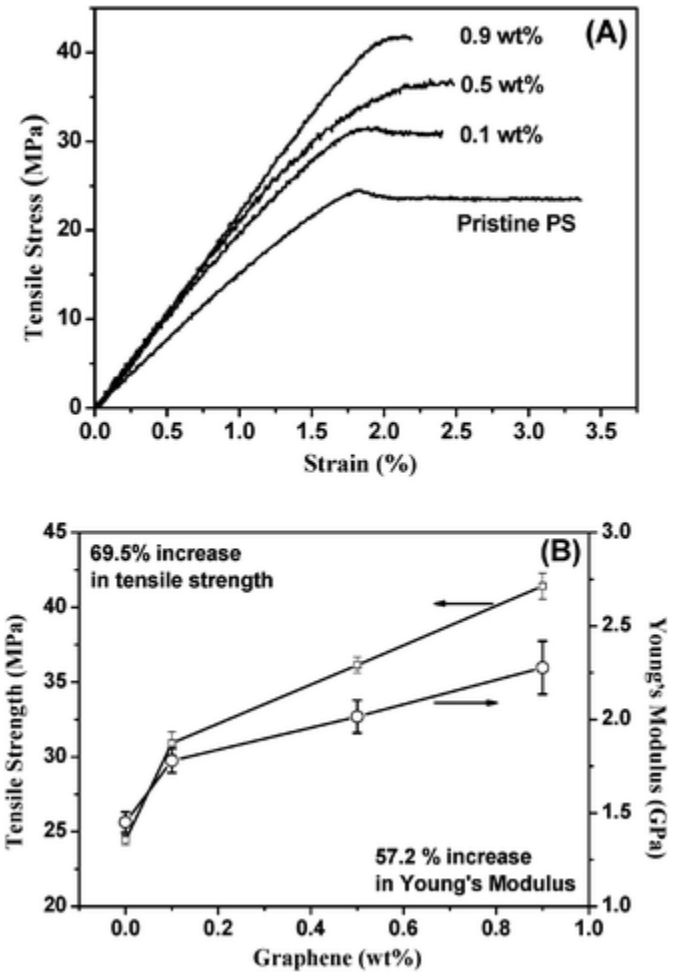

Fig. 10 (A) Representative stress-strain curves of the pristine PS and nanocomposite films with different contents of graphene sheets. (B) Young's modulus and tensile strength changes with increasing graphene content.

Such mechanical improvements are significant compared to the results reported in the literature,[31] which could be attributed to the efficient load transfer between graphene sheets and the PS matrix. Graphite sheets have been attempted to improve the mechanical properties of polymers, however, only moderate enhancements were observed in those systems. For example, when 5 wt% of thermally reduced graphene oxide sheets were added to styrene-acrylonitrile copolymer (SAN), only 34.5% of increases in EY were reported.[32] In this regard, poor particle dispersion and interface interaction are presumably responsible for the limited performance improvement. This is in contrast

Please cite this article as: M. Fang, K. Wang, H. Lu, Y. Yang, and S. R. Nutt, **"Covalent Polymer Functionalization of Graphene Nanosheets and Mechanical Properties of Composites"**, J. Mater. Chem. 19 (2009) 7098-7105. DOI:**http://dx.doi.org/10.1039/b908220d**

with the pronounced mechanical enhancements observed in graphene oxide-poly(vinyl alcohol) (PVA) systems, where the PVA nanocomposite with 0.7 wt% graphene oxide sheets revealed 76% and 62% increases in EY and σs.[33] The superior hydrophilicity of graphene oxide is conducive to their dispersion and interaction with PVA. This is distinct from the case in the present graphene-PS systems (PS is a non-polar polymer), in which both dispersion and interface interaction (or load transfer efficiency) were mediated by PS chains covalently bonded to the graphene surface.

It may be interesting to discuss the reinforcement effect of graphene- and carbon nanotube (CNT)-PS nanocomposites. Similarly, the early studies did not reveal remarkable mechanical improvements due to the bundling and entanglement of CNTs as well as poor load transfer efficiency.[11b,34] However, with resolution of these issues recent results revealed attractive mechanical enhancements, where the addition of 0.06 wt% SWNTs resulted in 82% and 78% of increases in tensile strength and elastic modulus of the PS composite films, respectively.[11a] Two causes are presumably responsible for the difference between CNTs and graphene sheets. One of them is that there exist more defects in the present graphene sheets because the oxidation took place during the functionalization. Although the reduction by hydrazine hydrate can partially restore the aromatic structure of graphene oxide, the residual defects still decrease the mechanical strength of reduced graphene sheets. The other is the difference in aspect ratio of two particles, which gives rise to an increase of critical threshold to establish a percolated particle network in matrices.[28c,d] The aspect ratio of CNTs is typically several hundreds or over one thousand[35] while the aspect ratio of the present graphene sheets is 20–40 if assuming 1 nm thick monolayer graphene sheets. Smaller aspect ratios require higher particle loadings to form percolated networks.[28,35] As a result, it is

Please cite this article as: M. Fang, K. Wang, H. Lu, Y. Yang, and S. R. Nutt, **"Covalent Polymer Functionalization of Graphene Nanosheets and Mechanical Properties of Composites"**, J. Mater. Chem. 19 (2009) 7098-7105. DOI:**http://dx.doi.org/10.1039/b908220d**

plausible for the present graphene sheets to exhibit a prominent mechanical reinforcement at a higher particle content than that of CNTs.

4. Conclusion

We have demonstrated an efficient method to covalently graft PS chains onto the surface of small graphene sheets (20–40 nm in diameter), which resulted in a grafting content as high as 82 wt% and a 15 °C enhancement in T_g. With the addition of only 0.9 wt% graphene sheets, the resulting PS composite film exhibited a prominent reinforcement effect, 57.2% and 69.5% increases in Young's modulus and tensile strength (relative to the pristine PS film), respectively. To our knowledge, this is the first report achieving covalent polymer functionalization of graphene by diazonium addition/ATRP and demonstrating the effect of functionalized graphene sheets on non-polar polymers such as PS. This protocol has broad application potential in graphene-based polymer nanocomposites, in particular because of the low cost of graphite and the versatility of both diazonium addition and ATRP. In efforts to optimize the structure and properties of polymer nanocomposites, particle dispersion and interface tailoring are crucial and are closely related to the size ratio of particles and polymer chains. The use of small graphene sheets offers several advantages compared to larger graphene sheets, including improved dispersion stability, reduced likelihood of introducing free volume into polymer hosts, and superior processability of polymer solutions (lower viscosity for example). The current work verifies the validity of these considerations. The smaller sheet size enabled us to disperse the reduced graphene sheets in solvents without adding a surfactant, which in turn made it possible to achieve a high grafting polymer density on the graphene surface. In this regard, a compromise may be required, for example, to prevent possible losses in electronic/electrical properties of graphene and derivative composites. A challenge for future

Please cite this article as: M. Fang, K. Wang, H. Lu, Y. Yang, and S. R. Nutt, **"Covalent Polymer Functionalization of Graphene Nanosheets and Mechanical Properties of Composites"**, J. Mater. Chem. 19 (2009) 7098-7105. DOI:**http://dx.doi.org/10.1039/b908220d**


research will be to functionalize larger graphene sheets, thereby providing dispersion and interface control in polymers.

Acknowledgements: This work was supported by the National Basic Research Program of China (Grant No. 2005CB623800), NSF of China (Grant No.50573014 and No.50773012), Shanghai Basic Research Program (Grant No.05JC14002). H. L. and Y. Y. also thank the support of NSFC program "Excellence in Research Group" (Grant No. 20221402).

References:

1 S. Park and R. S. Ruoff, Nat. Nanotechnol., 2009, 4, 217; D. Li and R. B. Kaner, Science, 2008, 320, 1170; A. K. Geim and K. S. Novoselov, Nat. Mater., 2007, 6, 183; C. G. Lee, X. D. Wei, J. W. Kysar and J. Hone, Science, 2008, 321, 385; A. K. Geim, Science, 2009, 324, 1530.
2 S. Stankovich, D. A. Dikin, G. H. B. Dommett, K. M. Kohlhaas, E. J. Zimney, E. A. Stach, R. D. Piner, S. T. Nguyen and R. S. Ruoff, Nature, 2006, 442, 282; T. Ramanathan, A. A. Abdala, S. Stankovich, D. A. Dikin, M. Herrera-Alonso, R. D. Piner, D. H. Adamson, H. C. Schniepp, X. Chen, R. S. Ruoff, S. T. Nguyen, I. A. Aksay, R. K. Prud'Homme and L. C. Brinson, Nat. Nanotechnol., 2008, 3, 327; D. A. Dikin, S. Stankovich, E. J. Zimney, R. D. Piner, G. H. B. Dommett, G. Evmenenko, S. T. Nguyen and R. S. Ruoff, Nature, 2007, 448, 457.
3 A. A. Balandin, S. Ghosh, W. Bao, I. Calizo, D. Teweldebrhan, F. Miao and C. N. Lau, Nano Lett., 2008, 8, 902.
4 K. S. Novoselov, A. K. Geim, S. V. Morozov, D. Jiang, Y. Zhang, S. V. Dubonos, I. V. Grigorieva and A. A. Firsov, Science, 2004, 306, 666; S. V. Morozov, K. S. Novoselov, M. I. Katsnelson, F. Schedin, D. C. Elias, J. A. Jaszczak and A. K. Geim, Phys. Rev. Lett., 2008, 100, 016602.
5 D. Dragoman and M. Dragoman, Appl. Phys. Lett., 2007, 91, 203116.
6 G. Mayer, Science, 2005, 310, 1144; A. C. Balazs, T. Emrick and T. P. Russell, Science, 2006, 314, 1107; L. S. Schadler, S. K. Kumar, B. C. Benicewicz, Sarah L. Lewis and S. E. Harton, MRS Bull., 2007, 32, 335.
7 Y. Y. Liang, D. Q. Wu, X. L. Feng and K. Mullen, Adv. Mater., 2009, 21, 1.
8 S. Stankovich, R. D. Piner, X. Q. Chen, N. Q. Wu, S. T. Nguyen and R. S. Ruoff, J. Mater. Chem., 2006, 16, 155.
9 S. Stankovich, R. D. Piner, S. T. Nguyen and R. S. Ruoff, Carbon, 2006, 44, 3342.
10 Y. F. Xu, Z. B. Liu, X. L. Zhang, Y. Wang, J. G. Tian, Y. Huang, Y. F. Ma, X. Y. Zhang and Y. S. Chen, Adv. Mater., 2009, 21, 1275, DOI: 10.1002/adma.200801617.
11 L. Xie, F. Xu, F. Qiu, H. B. Lu and Y. L. Yang, Macromolecules, 2007, 40, 3296; D. Qian, E. C. Dickey, R. Andrews and T. Rantell, Appl. Phys. Lett., 2000, 76, 2868.
12 S. Gupta, Q. L. Zhang, T. Emrick, A. C. Balazs and T. P. Russell, Nat. Mater., 2006, 5, 229.
13 Y. C. Si and E. T. Samulski, Nano Lett., 2008, 8, 1679; J. I. Paredes, S. Villar-Rodil, A. Martinez-Alonso and J. M. D. Tascon, Langmuir, 2008, 24, 10560; S. J. Park, J. H. An, I. H. Jung, R. D. Piner, S. J. An, X. S. Li, A. Velamakanni and R. S. Ruoff, Nano Lett., 2009, 9, 1593.

Please cite this article as: M. Fang, K. Wang, H. Lu, Y. Yang, and S. R. Nutt, **"Covalent Polymer Functionalization of Graphene Nanosheets and Mechanical Properties of Composites"**, J. Mater. Chem. 19 (2009) 7098-7105. DOI:**http://dx.doi.org/10.1039/b908220d**

14 H. J. Oh and P. F. Green, Nat. Mater., 2009, 8, 139; Y. J. Min, M. Akbulut, K. Kristiansen, Y. Golan and J. Israelachvili, Nat. Mater., 2008, 7, 527.
15 M. E. Mackay, A. Tuteja, P. M. Duxbury, C. J. Hawker, B. V. Horn, Z. B. Guan, G. H. Chen and R. S. Krishnan, Science, 2006, 311, 1740; L. Meli, A. Arceo and P. F. Green, Soft Matter, 2009, 5, 533; M. A. Yaklin, P. M. Duxbury and M. E. Mackay, Soft Matter, 2008, 4, 2441.
16 J. M. Kropka, V. Pryamitsyn and V. Ganesan, Phys. Rev. Lett., 2008, 101, 075702.
17 A. Tuteja, P. M. Duxbury and M. E. Mackay, Phys. Rev. Lett., 2008, 100, 077801.
18 J. R. Lomeda, C. D. Doyle, D. V. Kosynkin, W. F. Hwang and J. M. Tour, J. Am. Chem. Soc., 2008, 130, 16201.
19 W. S. Hummers and R. E. Offeman, J. Am. Chem. Soc., 1958, 80, 1339; S. Gilje, S. Han, M. Wang, K. L. Wang and R. B. Kaner, Nano Lett., 2007, 7, 3394; N. I. Kovtyukhova, P. J. Ollivier, B. R. Martin, T. E. Mallouk, S. A. Chizhik, E. V. Buzaneva and A. D. Gorchinskiy, Chem. Mater., 1999, 11, 771.
20 K. N. Kudin, B. Ozbas, H. C. Schniepp, R. K. Prud'homme, I. A. Aksay and R. Car, Nano Lett., 2008, 8, 36; I. Calizo, A. A. Balandin, W. Bao, F. Miao and C. N. Lau, Nano Lett., 2007, 7, 2645; D. Graf, F. Molitor, K. Ensslin, C. Stampfer, A. Jungen, C. Hierold and L. Wirtz, Nano Lett., 2007, 7, 238.
21 A. C. Ferrari and J. Robertson, Phys. Rev. B: Condens. Matter Mater. Phys., 2000, 61, 14095.
22 S. Stankovich, D. A. Dikin, R. D. Piner, K. A. Kohlhaas, A. Kleinhammes, Y. Y. Jia, Y. Wu, S. T. Nguyen and R. S. Ruoff, Carbon, 2007, 45, 1558.
23 H. Kong, C. Gao and D. Y. Yan, Macromolecules, 2004, 37, 4022.
24 G. M. Chen, S. H. Liu, S. J. Chen and Z. N. Qi, Macromol. Chem. Phys., 2001, 202, 1189; C. Y. Liang and S. Krimm, J. Polym. Sci., 1958, 29, 241.
25 A. V. Vivek and R. Dhamodharan, J. Polym. Sci., Part A: Polym. Chem., 2007, 45, 3818.
26 J. Pyun, T. Kowalewski and K. Matyjaszewski, Macromol. Rapid Commun., 2003, 24, 1043; J. Genzer and R. R. Bhat, Langmuir, 2008, 24, 2294; Y. Tsujii, K. Ohno, S. Yamamoto, A. Goto and T. Fukuda, Adv. Polym. Sci., 2006, 197, 1.
27 M. Husseman, E. E. Malmstrom, M. McNamara, M. Mate, D. Mecerreyes, D. G. Benoit, J. L. Hedrick, P. Mansky, E. Huang, T. P. Russell and C. J. Hawker, Macromolecules, 1999, 32, 1424; J. Pyun, S. J. Jia, T. Kowalewski, G. D. Patterson and K. Matyjaszewski, Macromolecules, 2003, 36, 5094.
28 H. B. Lu and S. Nutt, Macromolecules, 2003, 36, 4010; H. B. Lu and S. Nutt, Macromol. Chem. Phys., 2003, 204, 1832; L. An, Y. Z. Pan, X. W. Shen, H. B. Lu and Y. Y. Yang, J. Mater. Chem., 2008, 18, 4928; Y. Z. Pan, Y. Xu, L. An, H. B. Lu, Y. Y. Yang, W. Chen and S. Nutt, Macromolecules, 2008, 41, 9245.
29 A. Bansal, H. H. Yang, C. Z. Li, K. Cho, B. C. Benicewicz, S. K. Kumar and L. S. Schadler, Nat. Mater., 2005, 4, 693; P. Rittigstein, R. D. Priestley, L. J. Broadbelt and J. M. Torkelson, Nat. Mater., 2007, 6, 278.
30 M. K. Mukhopadhyay, X. Jiao, L. B. Lurio, Z. Jiang, J. Stark, M. Sprung, S. Narayanan, A. R. Sandy and S. K. Sinha, Phys. Rev. Lett., 2008, 101, 115501.
31 B. Debelak and K. Lafdi, Carbon, 2007, 45, 1727; T. Ramanathan, S. Stankovich, D. A. Dikin, H. Liu, H. Shen, S. T. Nguyen and L. C. Brinson, J. Polym. Sci., Part B: Polym. Phys., 2007, 45, 2097.
32 P. Steurer, R. Wissert, R. Thomann and R. Mulhaupt, Macromol. Rapid Commun., 2009, 30, 316.

Please cite this article as: M. Fang, K. Wang, H. Lu, Y. Yang, and S. R. Nutt, **"Covalent Polymer Functionalization of Graphene Nanosheets and Mechanical Properties of Composites"**, J. Mater. Chem. 19 (2009) 7098-7105. DOI:**http://dx.doi.org/10.1039/b908220d**

33 J. J. Liang, Y. Huang, L. Zhang, Y. Wang, Y. F. Ma, T. Y. Guo and Y. S. Chen, Adv. Funct. Mater., 2009, 19, 2297.
34 P. M. Ajayan, L. S. Schadler, C. Giannaris and A. Rubio, Adv. Mater., 2000, 12, 750.
35 M. Moniruzzaman and K. I. Winey, Macromolecules, 2006, 39, 5194.

Please cite this article as: M. Fang, K. Wang, H. Lu, Y. Yang, and S. R. Nutt, **"Covalent Polymer Functionalization of Graphene Nanosheets and Mechanical Properties of Composites"**, J. Mater. Chem. 19 (2009) 7098-7105. DOI:**http://dx.doi.org/10.1039/b908220d**